Science Translational Medicine
AAAS

www.sciencetranslationalmedicine.org/cgi/content/full/10/443/eaah6816/DC1

Supplementary Materials for

Ibrutinib inactivates BMX-STAT3 in glioma stem cells to impair malignant growth and radioresistance

Yu Shi, Olga A. Guryanova, Wenchao Zhou, Chong Liu, Zhi Huang, Xiaoguang Fang, Xiuxing Wang, Cong Chen, Qiulian Wu, Zhicheng He, Wei Wang, Wei Zhang, Tao Jiang, Qing Liu, Yaping Chen, Wenying Wang, Jingjing Wu, Leo Kim, Ryan C. Gimple, Hua Feng, Hsiang-Fu Kung, Jennifer S. Yu, Jeremy N. Rich, Yi-Fang Ping,* Xiu-Wu Bian,* Shideng Bao*

*Corresponding author. Email: baos@ccf.org (S.B.); bianxiuwu@263.net (X.-W.B.); pingyifang@126.com (Y.-F.P.)

Published 30 May 2018, *Sci. Transl. Med.* **10**, eaah6816 (2018)
DOI: 10.1126/scitranslmed.aah6816

This PDF file includes:

Materials and Methods

Isolation and culture of GSCs and NPCs

Glioma cells used in this study were derived from ten surgical biopsies of human GBM and were maintained as xenografts in immunodeficient mice. Human GBM surgical specimens were collected from the Neuro-Oncology Department of Southwest Hospital in Chongqing and Brain Tumor or Neuro-Oncology Center of Cleveland Clinic in accordance with an Institutional Review Board-approved protocol. GSCs were dissociated from xenografts or human GBM surgical specimens using the Papain Dissociation System (Worthington Biochemical) and were enriched for $CD133^+/CD15^+$ cells by fluorescence-activated cell sorting (FACS) as previously described (*4-6, 8*). Briefly, cells were labeled with a PE-conjugated anti-CD133 antibody (Miltenyi, 130-090-854) and a FITC-conjugated anti-CD15 antibody (BD Biosciences, 347423) at 4 °C for 40 minutes followed by FACS to isolate GSCs ($CD133^+/CD15^+$) and NSTCs ($CD133^-/CD15^-$). The sorted GSCs were cultured in Neurobasal medium (Gibco) supplemented with B-27 (Gibco), 20 ng/ml EGF (R&D), and 20 ng/ml b-FGF (R&D). The cancer stem cell phenotypes of GSCs were confirmed by the expression of multiple GSC markers (CD133, SOX2, and OLIG2) and functional assays (in vitro limiting dilution assay, serum-induced cell differentiation assay, and in vivo tumorigenic assay) to assess the self-renewal potential, multi-lineage differentiation potency, and in vivo tumorigenic capacity of GSCs as previously described (*4-6, 8*). These GSC lines were clustered as proneural, classical, or mesenchymal subtypes through RNA-sequencing (CapitalBio Technology and Genminix Informatics) according to the previously described glioblastoma transcriptional subtype classifications *(29, 38)*. Two human NPCs (15167 and 17231, Lonza) derived from human fetal brains and one human embryonic stem cell-derived NPC line (ENSA, Millipore) were cultured in Corning hESC Matrigel-coated dishes in the Neurobasal medium with B-27 (Gibco), 20 ng/ml EGF (R&D), and 20 ng/ml b-FGF (R&D). All cells used in this study were authenticated by karyotype analysis or short tandem repeat analysis and were verified to be free of mycoplasma contamination by PCR analysis as previously described (*39*).

In vitro cell viability and apoptosis assays

Cells were seeded in 96-well plates (1000 cells/ well) and treated with/without ibrutinib (Selleckchem, S2680) or stattic (Selleckchem, S7024) at the indicated concentration. Cell viability was determined at Day 0, Day 2, Day 4, and Day 6 using Cell Titer-Glo luminescent cell viability kit (Promega) according to the manufacturer's instructions. The EC_{50} of ibrutinib for GSCs and NPCs were determined by exposing cells to ibrutinib or vehicle control (DMSO) with 2-fold increasing concentrations from 0.1 to 25.6 μM. Cell viability was measured at 72 hours after treatment. Cell apoptosis induced by ibrutinib treatment was evaluated using the Annexin V-FITC Apoptosis Detection Kit (BD Pharmingen) on a BD LSR-II flow cytometer based on the manufacturer's guidance.

Sphere formation assay and in vitro limiting dilution assay

For the sphere formation assay, cells were seeded in 96-well plates at a density of 1000 cells/well and maintained in the Neurobasal medium with/without indicated doses of ibrutinib at 37 °C. Tumorsphere sizes and sphere numbers were assessed using EVOS FL microscope (AMG) on the 7th day after implantation. For in vitro limiting dilution assays, cells were plated in 96-well plates at 1, 5, 10, 20, 40, or 80 cells per well, with 10 replicates for each cell number. The presence of tumorspheres in each well was determined after 7 days of maintenance. Limiting dilution analysis was performed using online software (http://bioinf.wehi.edu.au/software/elda/) (*40*).

IL-6 stimulation assay

For IL-6 stimulation assays, attached cultured GSCs or NPCs were starved in Neurobasal medium without B-27 or growth factors for 14 hours, followed by treatment with recombinant human IL-6 (10 ng/ml, R&D) for the indicated amounts of time. Cells were harvested for co-immunoprecipitation and immunoblot assays or fixed in 4% paraformaldehyde for immunofluorescence staining.

Plasmid construction and lentivirus production

Lentiviral plasmids expressing shBMX or shSOCS3 and control non-targeting shRNA (SHC002) were acquired from Sigma-Aldrich with the shRNA sequences listed in **table S3**. Lentiviral plasmids expressing

Flag-tagged wild-type BMX (BMX-WT), dominant negative BMX (BMX-DN), active BMX (BMX-C), or constitutively active STAT3 (STAT3-C) were constructed by Shanghai Sunbio Bio-Medicine Technology Co., Ltd. as previously described (*8*). Lentiviral vector expressing SOCS3 was generated by cloning the SOCS3 coding sequence into the multiple cloning site of pCDH-EF1-MCS-IRES-Neo vector (System Biosciences).

Co-immunoprecipitation and immunoblot analyses

For co-immunoprecipitation, cells were harvested and lysed on ice for 20 minutes in buffer containing 50 mM Tris-HCl, pH 7.4, 150 mM NaCl, 5 mM EDTA, 10% glycerol, 1% NP-40, 1 mM sodium fluoride, and 1 mM sodium orthovanadate. Cell lysates from each sample were incubated with 5 μg of anti-JAK2 (Cell Signaling, #3230), anti-BMX (Abcam, ab73887), anti-gp130 (Millipore, #06-291), anti-STAT3 (Cell Signaling, #9139) or IgG control antibodies (Santa Cruz, sc-2025 or sc-2027) and Protein A/G Plus Agarose beads (Santa Cruz, sc-2003) for 14 hours at 4°C with constant rotation. Immunocomplexes captured by agarose beads were washed 3 times with 0.1% Triton X-100 in PBS and eluted by boiling in Laemmli buffer. Immunoblot assay was performed as previously described (*4-6, 8*). Antibodies used for immunoblot assays were as follows: anti-STAT3 (Cell Signaling, #9139, 1: 1000), anti-pSTAT3-Y^{705} (Cell Signaling, #9131, 1:1000), anti-JAK2 (Cell Signaling, #3230, 1: 1000), anti-pJAK2 (Cell Signaling, #3776, 1: 500), anti-gp130 (Millipore, #06-291, 1: 500), anti-BTK (Cell Signaling, #3533, 1: 1000), anti-BMX (Abcam, ab59360, 1:1000), anti-pBMX-Y^{40} (Cell Signaling, #3211, 1:1000 or ThermoFisher Scientific, PA5-36787, 1:500), anti-PARP (Cell Signaling, #9532, 1: 1000), anti-caspase-3 (Cell Signaling, #9665, 1: 1000), anti-cleaved caspase-3 (Cell Signaling, #9661, 1: 500), anti-SOX2 (Cell Signaling, #3579, 1:1000), anti-CD133 (Miltenyi, 130-092-395, 1:100), anti-OLIG2 (Millipore, MABN50, 1:2000), anti-OCT4 (Cell Signaling, #2750, 1:1000), anti-NANOG (Cell Signaling, #4903, 1:1000), anti-SOCS3 (Biolegend, 626601, 1 : 1000), anti-MGMT (Abcam, ab108630, 1:500), anti-Flag (Sigma-Aldrich, F1804, 1:1000 or Bioss, bs-0965R, 1:2000), anti-tubulin (Sigma-Aldrich, T6074, 1:10000 or Boster Biological Technology, #A01857-1, 1:2000), and anti-GAPDH (R&D, #686613, 1: 5000).

Immunofluorescent analyses

For immunofluorescent analysis, sections of mouse brain containing GBM xenografts or primary GBMs were fixed in 4% formaldehyde for 15 minutes, blocked in 1% BSA with or without 0.3% Triton X-100 for 1 hour, and then incubated with primary antibodies including anti-SOX2 (Santa Cruz, SC-17320, 1:100 or Millipore, MAB4423, 1:200), anti-Ki67 (Abcam, ab15580, 1:200), and anti-cleaved caspase-3 (Cell Signaling, #9661, 1:200) overnight. Slides with the tissue sections were then incubated with secondary antibodies labeled with AlexaFluor 488 or 567 (Invitrogen, 1:200) and 4',6-diamidino-2-phenylindole (DAPI, Beyotime), and mounted in Fluoromount G (Southern Biotech). Immunofluorescent staining of pSTAT3-Y^{705} in GSCs was performed using anti-pSTAT3-Y^{705} antibody (Cell Signaling, #9145, 1:100) according to the manufacturer's protocol. The SVZ was defined as a closely packed cell population along the lateral wall of the lateral ventricle, including those in the dorsolateral corner of the ventricle. NPCs in the SVZ of lateral ventricles were analyzed in three discrete coronal sections distributed from 0.74 mm rostral to the vertical zero plane at bregma point (a landmark visible on the skull) according to the Mouse Brain Atlas (http://www.mbl.org/atlas170/atlas170_frame.html). For each coronal section, five 40 × objective areas (386 × 386 μm^2) were analyzed to count NPCs marked by SOX2 in the SVZ of lateral ventricles using Leica SP5 microscope. The percentages of positive cells were calculated as the ratio of positive cells versus the total number of cells in the lateral ventricular walls of the SVZ in each field.

Immunohistochemical (IHC) analyses

IHC staining was performed using Dako REAL EnVision Detection System according to the manufacturer's protocol (DAKO). Primary antibodies used for IHC were anti-pBMX-Y^{40} (ThermoFisher Scientific, PA5-36787, 1:50), anti-BMX (BD, 610792, 1:100), anti-cleaved caspase-3 (Cell Signaling, #9661, 1:200), and anti-pSTAT3-Y^{705} antibody (Cell Signaling, #9145, 1:100). The images were captured using a Leica DM4000B microscope equipped with a QImaging EXi Aqua camera. Quantification of BMX and pBMX was performed by calculating the percentage of positive staining areas versus the whole areas in five randomly selected fields using Image J software (National Institutes of Health). The percentage of $pSTAT3^+$ cells and cleaved $caspase\text{-}3^+$ cells was quantified in five randomly selected fields using Image Pro Plus software (Media Cybernetics).

Establishment of GSC-derived intracranial GBM xenografts and ibrutinib treatment

Orthotopic GBM xenografts were established through intracranial transplantation of GSCs as described previously (*4-6, 8*). Animal experiments were performed using 4- to 6-week-old nonobese diabetic/severe combined immunodeficiency (NOD/SCID) mice from Laboratory Animal Centre at Southwest Hospital or NOD/SCID gamma (NSG) mice from Jackson Laboratories under a protocol approved by the Animal Research Committee of Southwest Hospital or Cleveland Clinic. Five thousand human GSC cultures (D456, T4121, or T387) expressing luciferase were injected into the right frontal lobe of mice. Mice in each group were treated with one of the following: vehicle control (i.p.), ibrutinib (25 mg/kg, i.p., Selleckchem, S2680), TMZ (65 mg/kg for 5 days, i.p., Selleckchem, S1237), radiation (5 × 2 Gy), or the combination of ibrutinib and radiation starting on the 7^{th} day after tumor implantation. Irradiation was performed with an X-ray irradiator (Rad Source Technologies, RS-2000). Anesthetized mice were placed in lead jigs through which the tumor implantation site was exposed for fractionated radiation. Xenograft growth was monitored by bioluminescent imaging using In Vivo Imaging System (IVIS) Spectrum (Perkin-Elmer). Mice were sacrificed at the indicated time points or upon manifestation of neurological symptoms.

Supplementary Figures

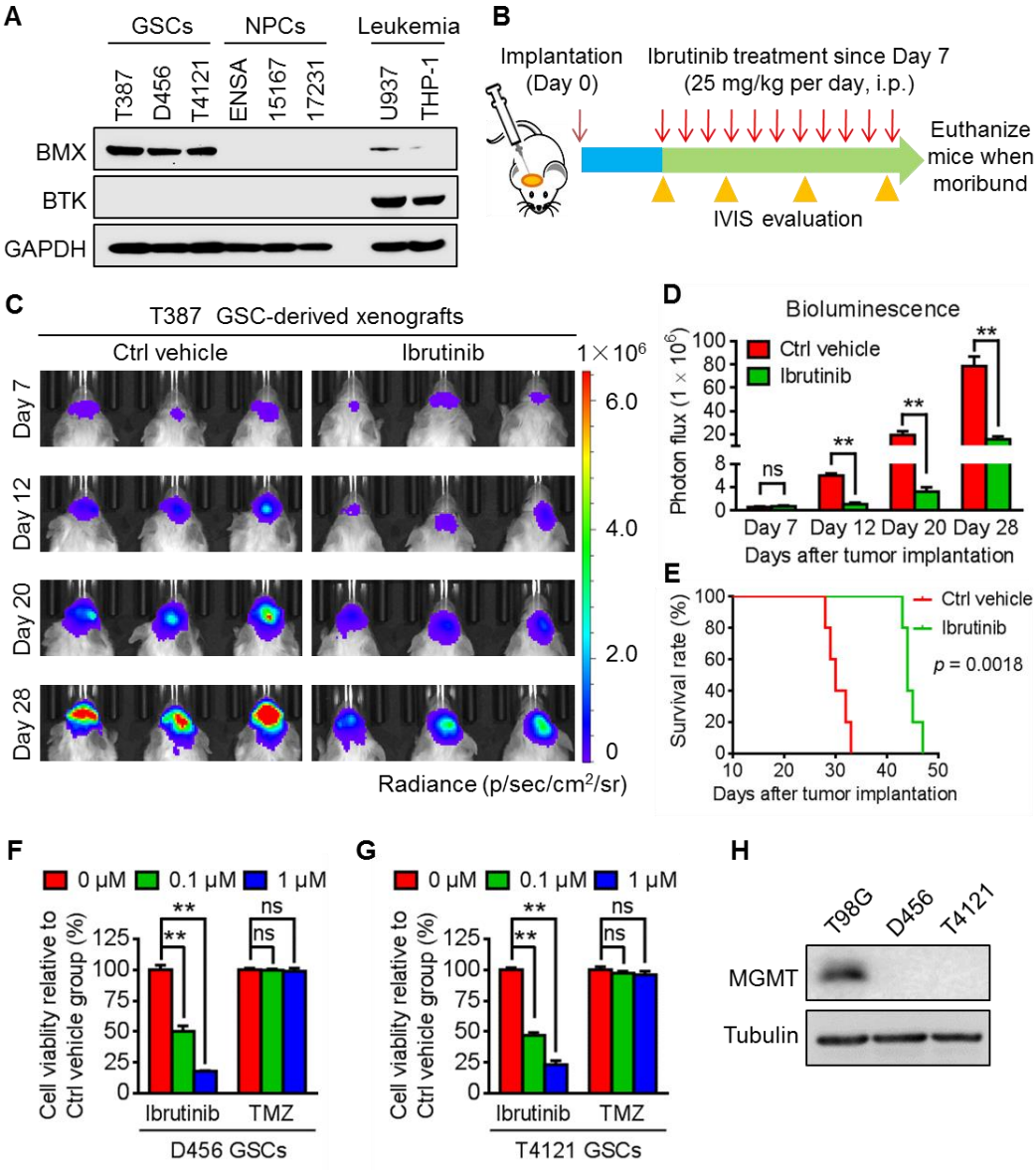

Fig. S1. Ibrutinib treatment inhibits GBM growth and prolongs animal survival.

(**A**) Immunoblot analyses of BMX, BTK, and GAPDH in human GSCs, NPCs, and leukemia cells. Expression of BMX and BTK in leukemia cell lines (U937 and THP-1) was used as positive control.

(**B**) Schematic diagram of ibrutinib treatment in mice bearing GSC-derived xenografts. Human GSCs (D456) expressing luciferase were transplanted into the brains of mice through intracranial injection to establish orthotopic xenografts. Seven days after tumor implantation, mice were treated with ibrutinib until mice became moribund. Tumor growth was monitored using the IVIS after tumor implantation.

(**C-D**) In vivo bioluminescent images (**C**) and the quantification (**D**) of orthotopic xenografts derived from T387 GSCs in mice treated with ibrutinib or the vehicle control at the indicated time points.

(**E**) Kaplan-Meier survival analysis of mice bearing GSC-derived xenografts (T387) treated with ibrutinib or the vehicle control.

(**F-G**) In vitro cell viability analyses of D456 GSCs (**F**) and T4121 GSCs (**G**) treated with different doses of ibrutinib or TMZ.

(**H**) Immunoblot analyses of MGMT in GSCs (D456 and T4121) and T98G GBM cells. Expression of MGMT in T98G was used as a positive control.

Data are shown as means ± S.E.M (**D**) or as means ± S.D (**F** and **G**). ns, not significant, $^{**}p < 0.01$. i.p., intraperitoneal injection; p, photons; sec, second; sr, steradian.

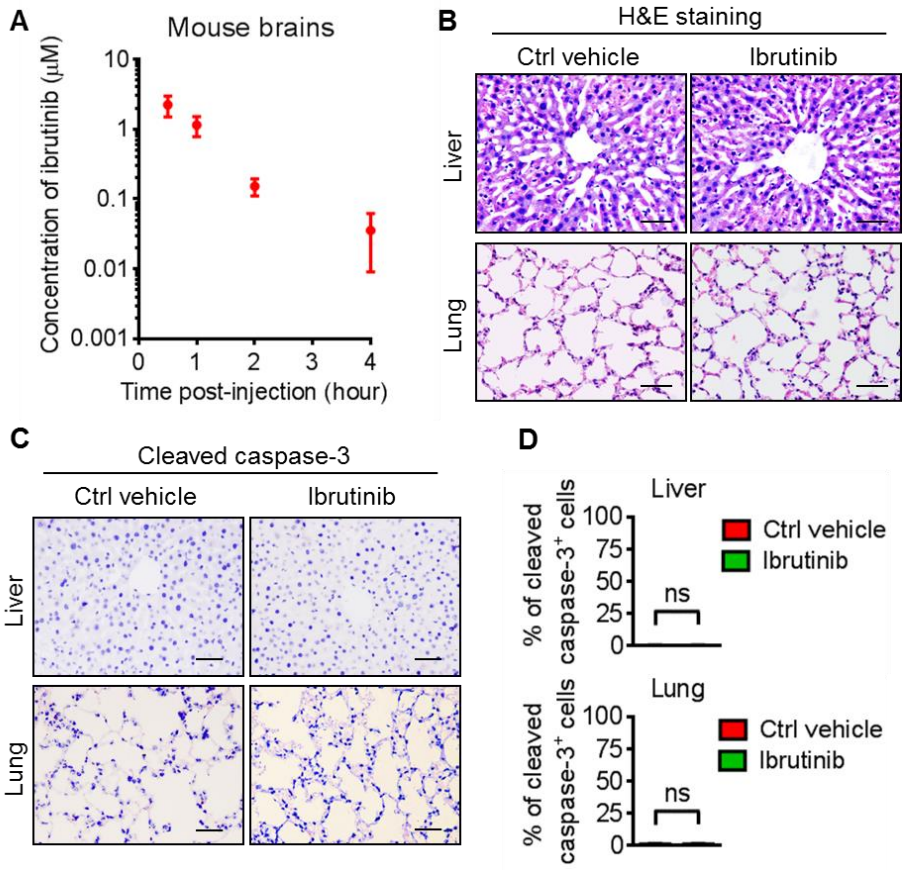

Fig. S2. Ibrutinib penetrates into mouse brains and has no severe systemic side effects.

(**A**) Concentration of ibrutinib in mouse brains after intraperitoneal injection.

(**B**) Representative H&E images of liver and lung tissues of mice treated with ibrutinib or the vehicle control.

(**C**-**D**) Representative IHC images of cleaved caspase-3 (**C**) and the proportion of cleaved caspase-3$^+$ cells (**D**) in mouse liver and lung tissues with indicated treatments.

Data are shown as means ± S.D. ns, not significant. Scale bar, 100 μm.

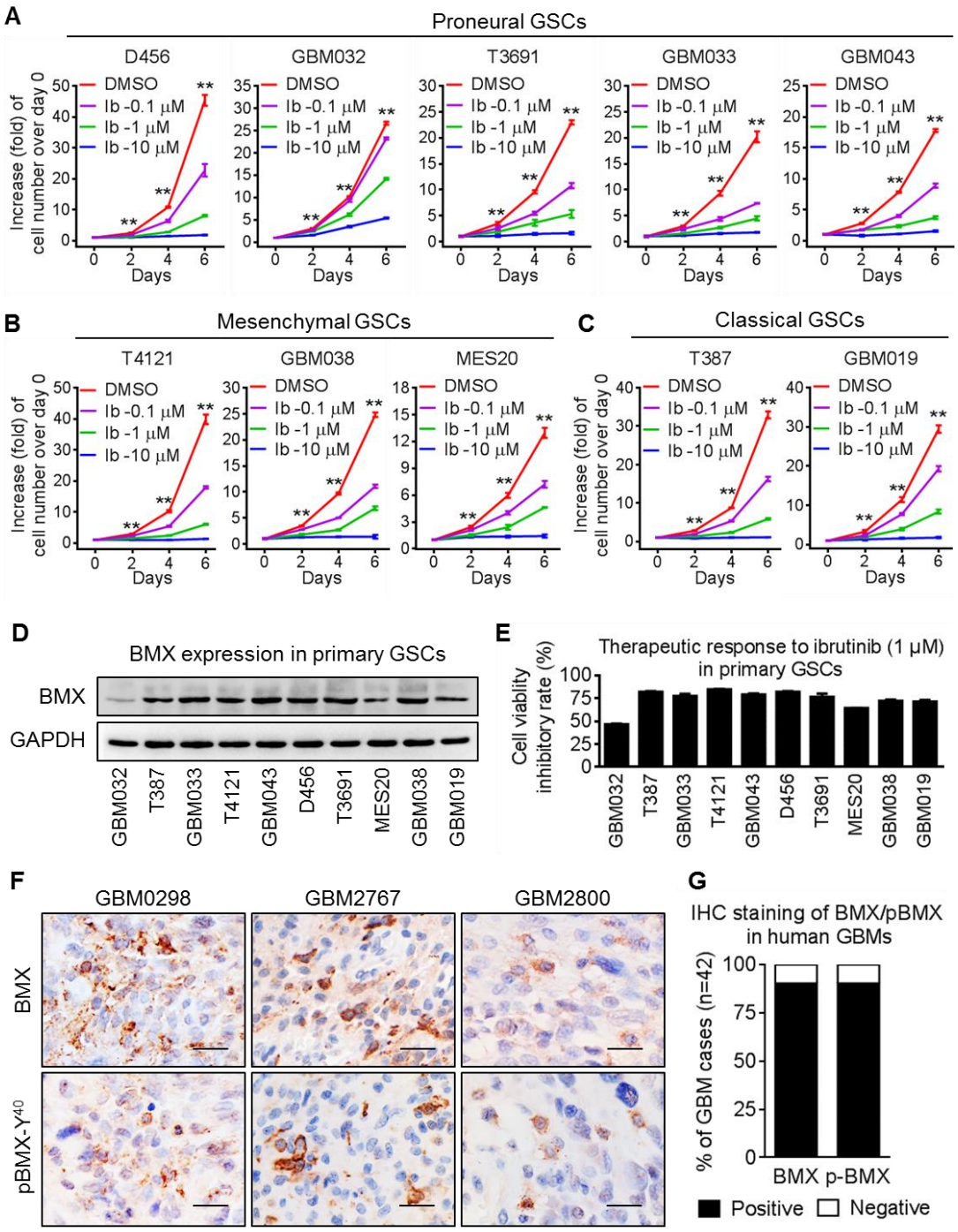

Fig. S3. Ibrutinib treatment is effective for most GBMs tested.

(**A-C**) In vitro cell viability assay of human GSC lines treated with different doses of ibrutinib (0.1 μM, 1 μM, and 10 μM) or the vehicle control. The GSC lines were clustered as proneural (**A**), mesenchymal (**B**), or classical (**C**) subtypes according to the glioblastoma transcriptional subtype analysis.

(**D**) Immunoblot analyses of BMX and GAPDH in primary GSCs.

(**E**) In vitro cell viability analyses showing the therapeutic response to ibrutinib in primary GSCs.

(**F**) IHC of BMX (upper panel) and pBMX-Y^{40} (lower panel) in human GBM tissues.

(**G**) Quantifications of the percentage of human GBMs expressing BMX or pBMX -Y^{40} in the tested GBM cohort (n = 42 cases).

Data are shown as means ± S.D. $^{**}p < 0.01$. Ib, ibrutinib. Scale bar, 40 μm.

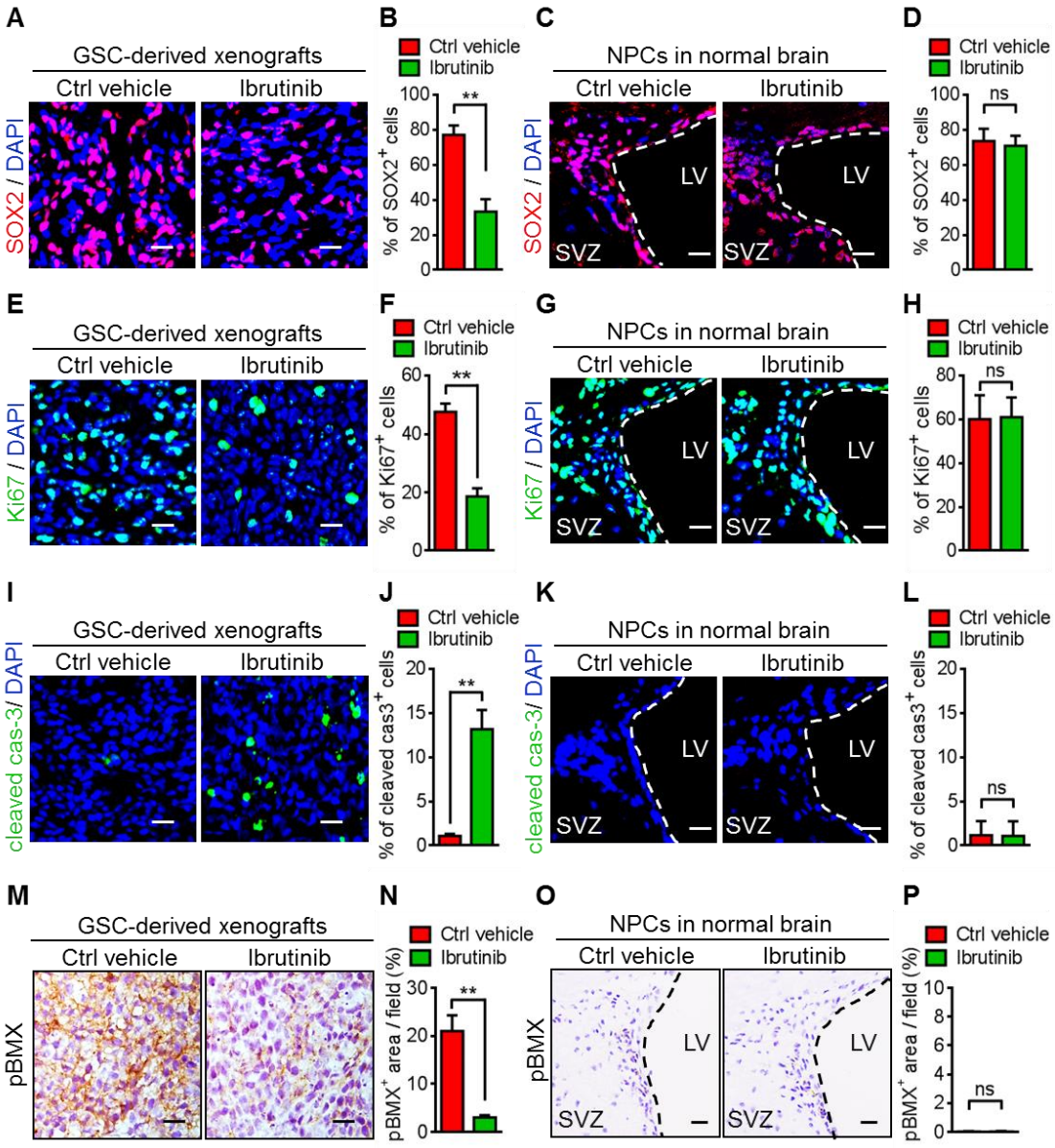

Fig. S4. Ibrutinib treatment targets GSCs but not NPCs in vivo.

(**A-B**) Representative immunofluorescent images (**A**) and the quantification (**B**) of human GSC populations positive for SOX2 (red) in xenografts treated with ibrutinib or the vehicle control.

(**C-D**) Representative immunofluorescent images (**C**) and the quantification (**D**) of mouse NPCs positive for SOX2 (red) in the SVZ of mouse brains with indicated treatments.

(**E-F**) Representative immunofluorescent images (**E**) and the quantification (**F**) of $Ki67^+$ tumor cells (green) in xenografts with indicated treatments.

(**G-H**) Representative immunofluorescent images (**G**) and the quantification (**H**) of $Ki67^+$ cells (green) in the SVZ of mouse brains with indicated treatments.

(**I-J**) Representative immunofluorescent images (**I**) and the quantification (**J**) of cleaved caspase-3 (green) in xenografts with indicated treatments.

(**K-L**) Representative immunofluorescent images (**K**) and the quantification (**L**) of cleaved caspase-3 (green) in the SVZ of mouse brains with indicated treatments.

(**M-N**) Representative IHC images (**M**) and the quantification (**N**) of pBMX signal in D456 GSC-derived xenografts with indicated treatments. Quantification of pBMX was performed by calculating the percentage of positive staining area to the whole area in five randomly-selected fields.

(**O-P**) Representative IHC images (**O**) and the quantification (**P**) of pBMX signal in the SVZ of mouse brains with indicated treatments.

Data are shown as means ± S.D. ***p* < 0.01. ns, not significant. n = 5 for each group. SVZ, subventricular zone; LV, lateral ventricle. The percentages of indicated positive cells are the ratio of positive cells to the total number of cells in xenografts (**B**, **F,** and **J**) or in the entire SVZ region of the lateral ventricle (**D**, **H,** and **L**) in each field. Scale bar, 25 μm (**A**, **C**, **E**, **G**, **I**, **K**, and **M**) or 50 μm (**O**).

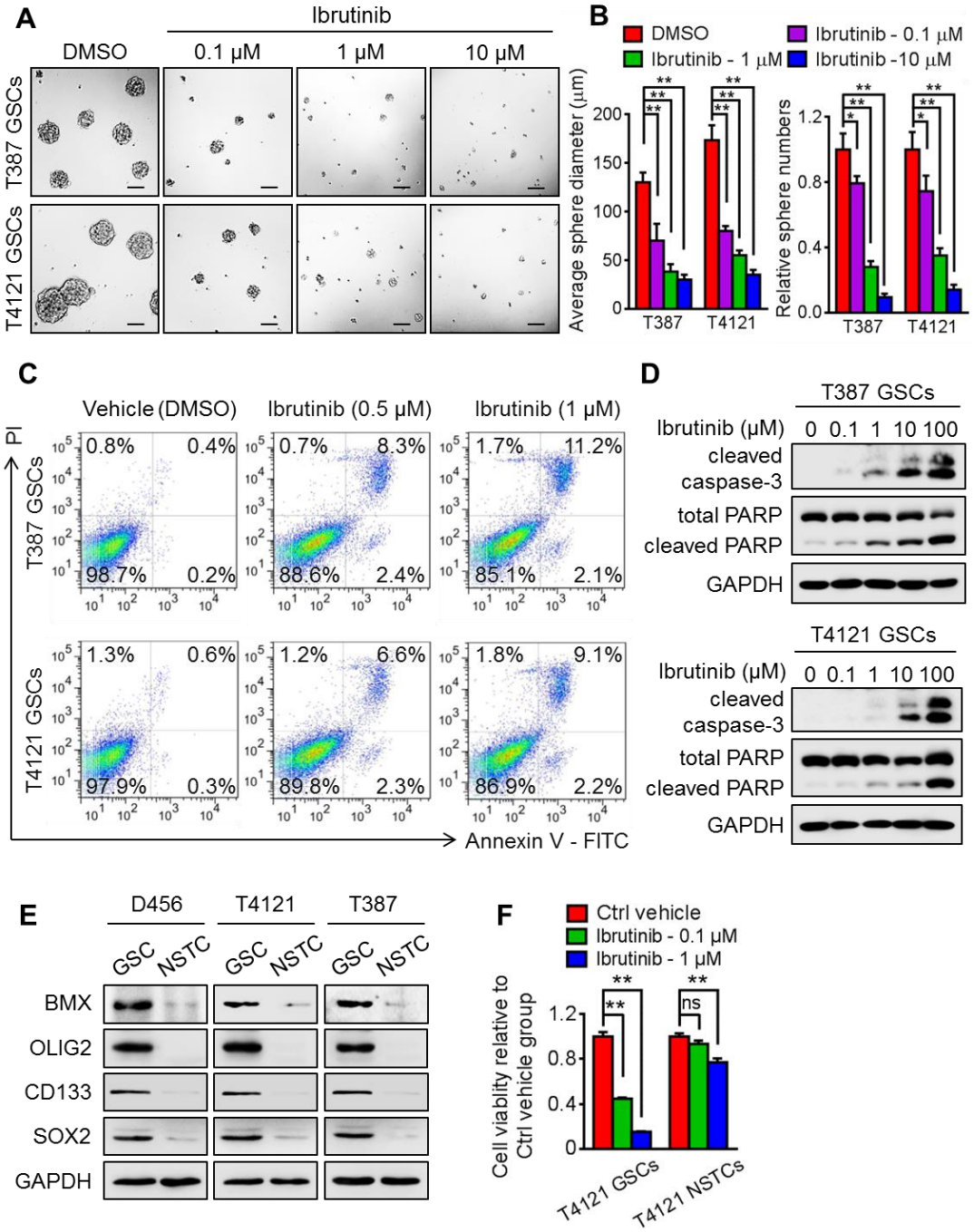

Fig. S5. Ibrutinib is more effective at targeting GSCs than NSTCs.

(**A-B**) Representative images of GSC tumorspheres (**A**) and the quantification of sphere diameter (**B**, left panel) and number (**B**, right panel) for T387 and T4121 GSCs treated with indicated doses of ibrutinib or the vehicle control.

(**C**) Cell apoptosis analyses of GSCs (T387 and T4121) treated with different doses of ibrutinib or the vehicle control.

(**D**) Immunoblot analyses of the apoptosis markers cleaved caspase-3, cleaved PARP, PARP, and GAPDH in GSCs (T387, upper panel; T4121, lower panel) treated with indicated doses of ibrutinib or the vehicle control.

(**E**) Immunoblot analyses of BMX, GSC markers (OLIG2, CD133, and SOX2), and GAPDH in D456, T4121, and T387 GSCs and NSTCs.

(**F**) In vitro cell viability analyses of T4121 GSCs and NSTCs treated with indicated doses of ibrutinib or the vehicle control.

Data are shown as means ± S.D. ns, not significant, *$p < 0.05$; **$p < 0.01$. Scale bar, 100 μm.

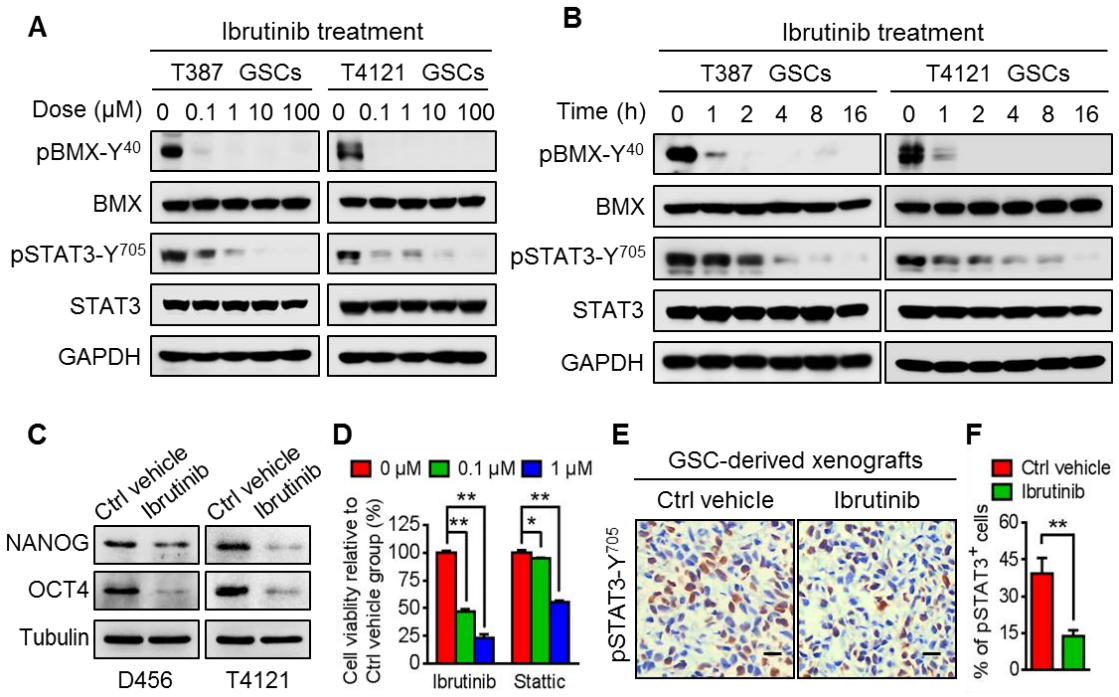

Fig. S6. Ibrutinib treatment inhibits BMX-mediated STAT3 activation in GSCs.

(**A**) Immunoblot analyses of pBMX-Y^{40}, BMX, pSTAT3-Y^{705}, STAT3, and GAPDH in T387 and T4121 GSCs treated with indicated doses of ibrutinib or the vehicle control.

(**B**) Immunoblot analyses of pBMX-Y^{40}, BMX, pSTAT3-Y^{705}, STAT3, and GAPDH in T387 and T4121 GSCs treated with ibrutinib for varied amounts of time (0 hour, 2 hours, 4 hours, 8 hours, and 16 hours).

(**C**) Immunoblot analyses of NANOG and OCT4 in D456 and T4121 GSCs with indicated treatments.

(**D**) In vitro cell viability analyses of T4121 GSCs treated with different doses of ibrutinib or STAT3 inhibitor stattic.

(**E-F**) Representative IHC images (**E**) and the quantification of pSTAT3-Y^{705} (**F**) in the D456 GSC-derived xenografts with indicated treatments. n = 5 for each group. Data are shown as means ± S.D. *p < 0.05, **p < 0.01. Scale bar, 25 μm.

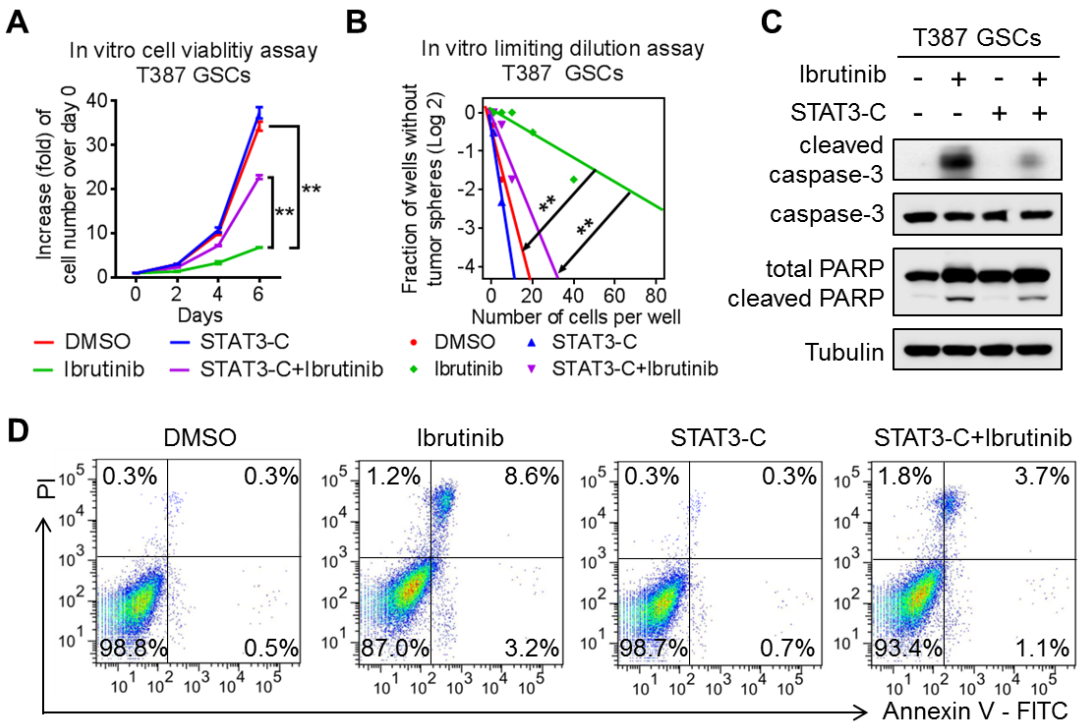

Fig. S7. Ectopic expression of constitutively active STAT3 largely rescues GSC maintenance disrupted by ibrutinib.

(**A**) In vitro cell viability assay of STAT3-C-expressing T387 GSCs treated with ibrutinib or the vehicle control.

(**B**) In vitro limiting dilution assay of STAT3-C-expressing T387 GSCs treated with ibrutinib or the vehicle control.

(**C**) Immunoblot analyses of the apoptosis markers cleaved caspase-3, caspase-3, cleaved PARP, PARP, and tubulin in STAT3-C-expressing T387 GSCs treated with ibrutinib or the vehicle control.

(**D**) Cell apoptosis analyses of STAT3-C-expressing T387 GSCs treated with ibrutinib or the vehicle control.

Data are shown as means ± S.D. $^{**}p < 0.01$.

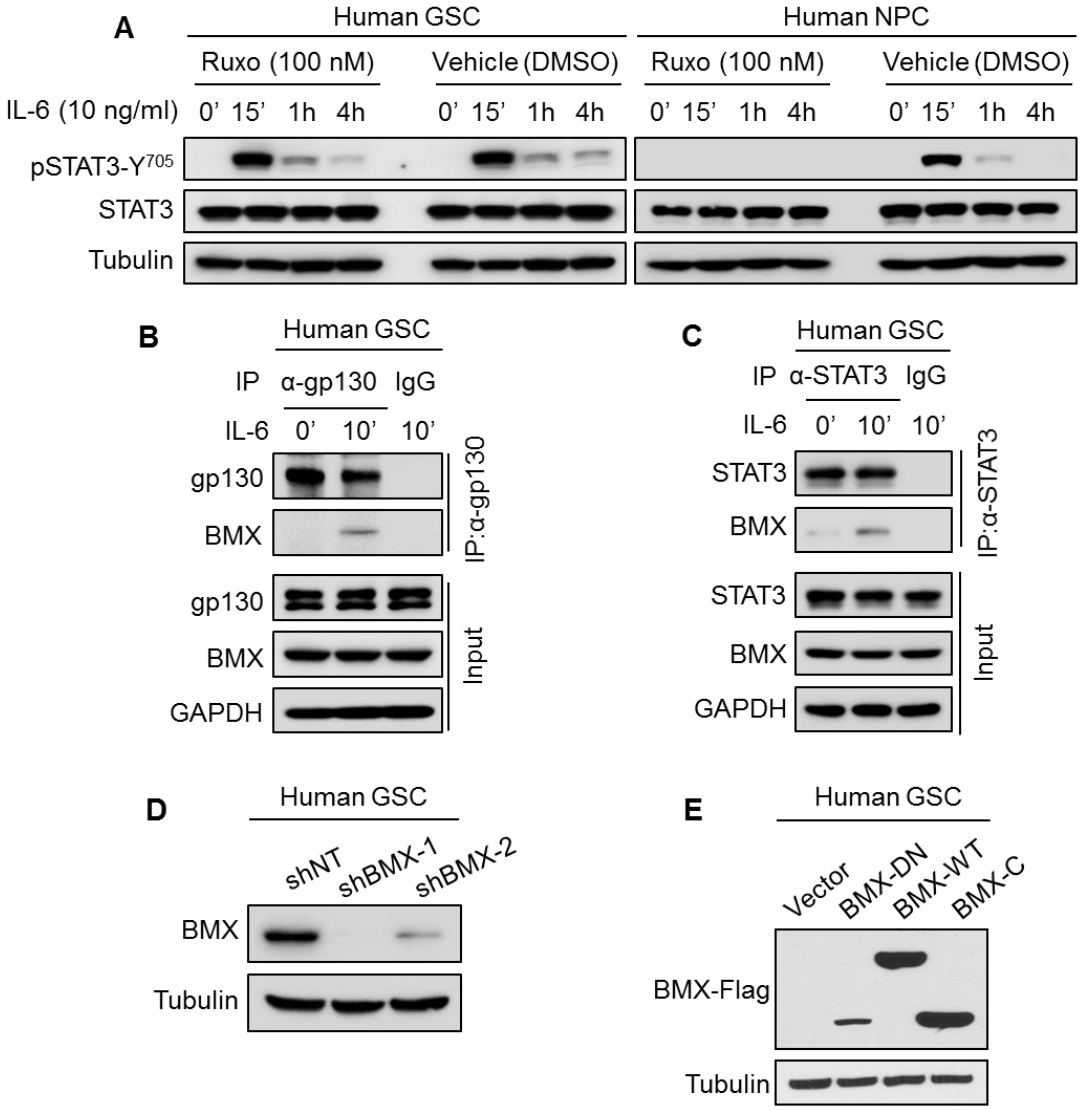

Fig. S8. JAK2 mediates STAT3 activation in NPCs, whereas BMX interacts with gp130 to mediate STAT3 activation in GSCs.

(**A**) Immunoblot analyses of pSTAT3-Y^{705}, STAT3, and tubulin in human GSCs (D456) and NPCs (15167) treated with the JAK2 inhibitor ruxolitinib or the vehicle control.

(**B**) Co-immunoprecipitation of BMX with anti-gp130 antibody in D456 GSCs. Precipitation with normal rabbit IgG was used as a negative control.

(**C**) Co-immunoprecipitation of BMX with anti-STAT3 antibody in D456 GSCs. Precipitation with normal mouse IgG was used as a negative control.

(**D**) Immunoblot analysis of BMX and tubulin in D456 GSCs expressing one of two shRNAs against BMX (shBMX) or control non-targeting shRNA (shNT) to confirm BMX knockdown.

(**E**) Immunoblot analyses of BMX-Flag and tubulin in D456 GSCs expressing a dominant negative form of BMX (BMX-DN), a wild-type BMX (BMX-WT), or a constitutively active BMX (BMX-C).

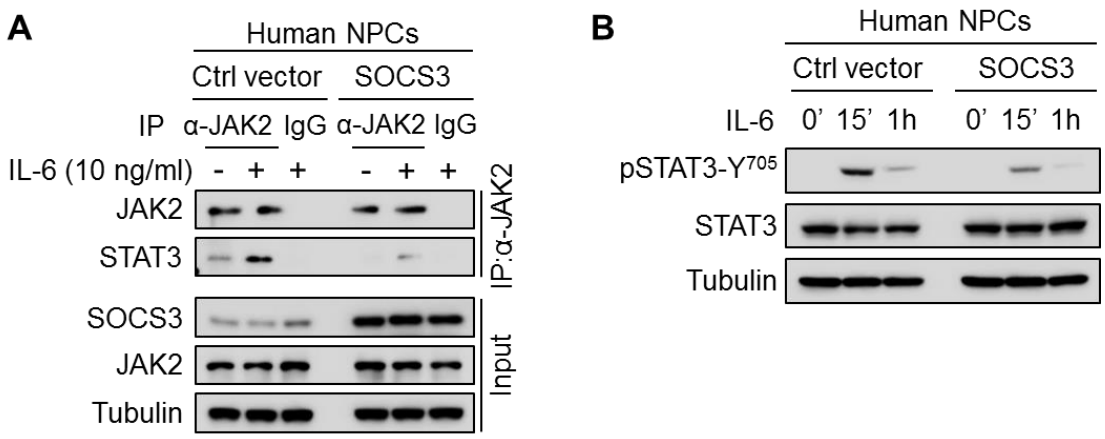

Fig. S9. Forced expression of SOCS3 inhibits JAK2-mediated STAT3 activation in NPCs.

(**A**) Co-immunoprecipitation of STAT3 with anti-JAK2 antibody in 15167 human NPCs transduced with SOCS3-expressing vector or the control vector. Precipitation with normal rabbit IgG was used as a negative control. Total cell lysates (input) were also immunoblotted with antibodies against SOCS3, JAK2, and tubulin.

(**B**) Immunoblot analyses of pSTAT3-Y^{705}, STAT3, and tubulin in 15167 NPCs transduced with SOCS3-expressing vector or the control vector upon IL-6 stimulation (10 ng/ml).

Supplementary Tables

Table S1. Pathological and molecular features of patient-derived GSCs used in this study.

Case #	Histopathology	Grade	GBM subtype	IDH1/2 mutation	ATRX mutation
D456	GBM	IV	Proneural	(-)	(-)
T387	GBM	IV	Classical	(-)	(-)
T4121	GBM	IV	Mesenchymal	(-)	(-)
GBM032	GBM	IV	Proneural	(-)	(-)
MES20	GBM	IV	Mesenchymal	(-)	(-)
T3691	GBM	IV	Proneural	(-)	(-)
GBM043	GBM	IV	Proneural	(-)	(-)
GBM038	GBM	IV	Mesenchymal	(-)	(-)
GBM033	GBM	IV	Proneural	(-)	(-)
GBM019	GBM	IV	Classical	(-)	(-)

Abbreviations: GBM, glioblastoma; IDH 1/2, isocitrate dehydrogenase 1/2; ATRX, α-thalassemia / mental retardation, X-linked.

Table S2. Expression of BMX and pBMX-Y[40] and the pathological characteristics of human GBMs used in this study.

Specimen	WHO Grade	Gender	Age	Predominant lobe	% of BMX^+ area	% of $pBMX^+$ area	IDH1 mutation
GBM9643	IV	Male	63	Frontal	Negative	Negative	Negative
GBM1217	IV	Female	39	Frontal	30.87	6.63	Negative
GBM9281	IV	Male	59	Frontal	12.47	10.12	Negative
GBM9010	IV	Female	41	Frontal	Negative	Negative	Positive
GBM2953	IV	Male	47	Temporal	4.33	3.14	Negative
GBM7255	IV	Female	58	Parietal	5.77	1.90	Negative
GBM2800	IV	Male	38	Cerebellum	14.45	12.06	Negative
GBM3969	IV	Female	45	Temporal	33.54	20.92	Negative
GBM6694	IV	Male	44	Temporal	Negative	Negative	Negative
GBM7204	IV	Male	33	Frontal	Negative	Negative	Negative
GBM8476	IV	Male	46	Frontal	29.96	18.41	Negative
GBM2689	IV	Female	38	Temporal	6.77	4.22	Negative
GBM2767	IV	Male	56	Temporal	21.12	15.81	Negative
GBM0298	IV	Male	68	Parietal	19.10	13.23	Negative
GBM7010	IV	Male	56	Temporal	7.37	5.96	Negative
GBM0729	IV	Male	50	Temporal	16.56	10.78	Negative
GBM0953	IV	Female	24	Parietal	25.37	21.68	Negative
GBM3369	IV	Male	62	Frontal	17.96	11.20	Negative
GBM6942	IV	Male	35	Temporal	10.98	8.17	Negative
GBM7219	IV	Female	68	Temporal	12.13	5.25	Negative
GBM9160	IV	Male	49	Occipital	14.84	12.30	Negative
GBM0194	IV	Female	51	Frontal	7.83	5.28	Positive
GBM1388	IV	Male	50	Temporal	8.06	4.64	Negative
GBM1979	IV	Male	45	Frontal	12.07	7.99	Negative
GBM2296	IV	Female	53	Frontal	11.11	6.81	Negative
GBM3737	IV	Female	21	Parietal	21.67	15.04	Negative
GBM5839	IV	Male	62	Frontal	17.05	14.43	Negative
GBM7549	IV	Male	56	Frontal	25.10	22.19	Negative
GBM0537	IV	Male	22	Parietal	20.52	16.45	Negative
GBM0935	IV	Male	79	Temporal	9.52	5.24	Negative
GBM1024	IV	Male	39	Frontal	6.89	4.32	Positive
GBM1054	IV	Female	43	Temporal	14.41	11.38	Positive
GBM1090	IV	Female	43	Frontal	10.46	7.90	Negative
GBM1091	IV	Male	57	Temporal	30.02	27.00	Negative
GBM2970	IV	Female	22	Parietal	8.37	5.04	Negative
GBM5190	IV	Male	37	Frontal	25.05	24.07	Negative
GBM8147	IV	Male	53	Temporal	24.57	17.85	Negative
GBM9131	IV	Female	28	Parietal	9.52	5.65	Negative
GBM9589	IV	Female	51	Parietal	10.32	6.37	Negative
GBM0169	IV	Female	42	Frontal	38.86	25.70	Negative
GBM0196	IV	Male	46	Temporal	26.97	21.32	Negative
GBM0658	IV	Male	35	Parietal	9.87	7.29	Negative

Abbreviations: GBM, glioblastoma; IDH1, isocitrate dehydrogenase 1.

Table S3. Sequences of shRNAs used in this study.

shRNA	Sequence
shNT	CCGGCAACAAGATGAAGAGCACCAACTCGAGTTGGTGCTCTTCATCTTGTTGTTTTT
shBMX-1	CCGGGCAATATGACAGCAACTCAAACTCGAGTTTGAGTTGCTGTCATATTGCTTTTT
shBMX-2	CCGGCCATTGAACCACTTCGGGAAACTCGAGTTTCCCGAAGTGGTTCAATGGTTTTT
shSOCS3-1	CCGGCCACCTGGACTCCTATGAGAACTCGAGTTCTCATAGGAGTCCAGGTGGTTTTTG
shSOCS3-2	CCGGCCGCTTCGACTGCGTGCTCAACTCGAGTTGAGCACGCAGTCGAAGCGGTTTTTG